Asymptotic and Non-Asymptotic Analysis of Uplink Sum Rate for Relay-Assisted MIMO Cellular Systems

Hao Wu, Liming Wang, *Member, IEEE*, Xiaodong Wang, *Fellow, IEEE*, and Xiaohu You, *Fellow, IEEE*

***Abstract*—We consider uplink relay-assisted MIMO cellular systems with multiple relays deployed in each cell that perform the amplify-and-forward operations. We are interested in obtaining deterministic expressions for the ergodic sum rate of such systems. We first consider the large MIMO dimension scenario, and obtain two asymptotic sum rate expressions, corresponding to the cases of fixed number of users and large number of users, respectively. We then consider the case of arbitrary MIMO dimension and large number of users, and obtain an upper and lower bound that the sum rate lies in between with high probability. The bounds are tight when the number of users is large. Both single-cell and multi-cell systems are considered, where the latter assumes full base station cooperation. Numerical experiments show that these deterministic sum rate expressions match well with the Monte Carlo simulation results. Therefore they can be useful tools for the design and analysis of relay-assisted MIMO cellular systems.**

***Index Terms*—Uplink sum rate, MIMO, relay, multi-cell, random matrix, asymptotic analysis, non-asymptotic analysis.**

I. Introduction

RELAY-ASSISTED cooperative communications have received significant recent interests due to their potential of enhancing the system throughput. Among the several existing relay strategies, the amplify-and-forward (AF) scheme is easy to implement and amenable to theoretical analysis. In particular, the rate of wireless AF systems is analyzed in [1]. In [2] and [3], the asymptotic rate of a MIMO AF system with finite number of relay hops is analyzed when the number of antennas is large. Optimal precoding at the source and relays is also discussed to maximize the asymptotic sum rate in [2]. However, these works consider only the case of a single transmitter and receiver, and the direct link from source to sink is ignored. On the other hand, the achievable rate of a MIMO relay system employing the AF strategy is discussed in [4]–[7] and [8], where the direct link from the source to the destination is considered. Furthermore, the ergodic capacity and the optimal input covariance matrix to achieve the capacity are analyzed in [9] with the presence of multiple relays and direct link.

In this paper, we are interested in computing the sum rate of an uplink MIMO AF system in a single-cell or multi-cell network with multiple relays. The multi-user capacities of uplink and downlink MIMO systems are given in [10]. More recently, multi-cell systems have been considered [11]. In [12], a multi-cell processing model is considered where a full BS cooperation strategy is employed resulting in an augmented multi-user model. The asymptotic sum rate for such system is then analyzed using the random matrix theory. Moreover, the sum rate of an uplink TDMA multi-cell system with non-regenerative AF relays is analyzed in [13], where it is assumed that the mobile users serve as relays to help each other. In this paper we are interested in systems with fixed relay stations that perform AF operations.

Specifically, we perform both asymptotic and non-asymptotic analyses on the sum rate for MIMO cellular communication systems employing fixed AF relay stations and multi-cell cooperation. We start from a single-cell uplink MIMO system with multiple AF relays and multiple users in Gaussian fading channels. The relays just amplify and forward the signals, and we consider precoding matrices at both users and relays. At the receiving end, the base station (BS) receives and combines signals from all users and all relays. All channel links including users to BS, users to relays and relays to BS (Fig. 1) are taken into account. In addition, the Kronecker model [14] is employed to model correlated MIMO channels. The asymptotic results that we obtain are useful in calculating the sum rate of a system with large number of antennas. On the other hand, the non-asymptotic results are useful for systems with any number of antennas and large number of users. Extension to multi-cell systems is also given.

The remainder of the paper is organized as follows. In Section II, we give the system model. In Section III, we provide two asymptotic analyses on the sum rate. The non-asymptotic analysis is given in Section IV. Numerical results are provided in Section V. Section VI contains the conclusion.

II. System Model

We start by considering a single-cell MIMO system with relays. Specifically, the cell has one BS at the center, K mobile users at random locations within the cell and M relays at some fixed positions. The amplify-and-forward (AF) strategy is adopted at each relay, where a precoding matrix is applied to

Manuscript received March 04, 2013; revised June 03, 2013 and June 20, 2013; accepted July 01, 2013. Date of publication July 24, 2013; date of current version February 21, 2014. The associate editor coordinating the review of this manuscript and approving it for publication was Prof. Jian-Kang Zhang. This work was supported in part by the Natural Science Foundation of China under grants 61221002 and 61101086 and 61329101.

H. Wu and X. You are with the National Communications Research Lab, Southeast University, Nanjing 210096, China (e-mail: haowu@seu.edu.cn; xhyu@seu.edu.cn).

L. Wang is with the Department of Electrical and Computer Engineering, Duke University, Durham, NC 27708 USA (e-mail: liming.w@duke.edu).

X. Wang is with the Electrical Engineering Department, Columbia University, New York, NY 10027 USA, and also with King Abdulaziz University, Jeddah, Saudi Arabia (e-mail: wangx@ee.columbia.edu).

Color versions of one or more of the figures in this paper are available online at http://ieeexplore.ieee.org.

Digital Object Identifier 10.1109/TSP.2013.2274642

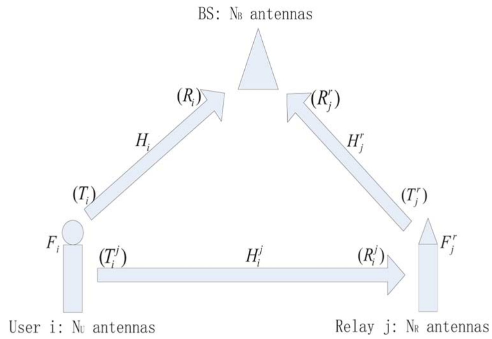

Fig. 1. An uplink single-cell MIMO system with relays.

	Slot 1	Slot 2
User	Tx: User Rx: Relay and BS	Idle
Relay	Idle	Tx: Relay Rx: BS

Fig. 2. The two-stage amplify-and-forward (AF) relay strategy.

the received signal which is then forwarded to the BS. The BS receives the signals from all users and all relays. Moreover, we assume perfect synchronization among the relays so that there is no interference among them.

The system model is depicted in Fig. 1, with various parameters annotated. Specifically, we assume that each user has N_U antennas, each relay has N_R antennas and the BS has N_B antennas. User i transmits information signal $\boldsymbol{x}_i$ through a precoding matrix $\boldsymbol{F}_i$, which is received by the BS and all relays. We assume unit transmit power, i.e., $\mathbb{E}\{\boldsymbol{x}_i^H\boldsymbol{x}_i\} = 1$. The channel matrix between user i and the BS is $\boldsymbol{H}_i$, and the channel matrix between user i and relay j is $\boldsymbol{H}_i^j$. Upon receiving the superposition of all user signals, relay j forwards it to the BS using a precoding matrix $\boldsymbol{F}_j^r$, and the channel matrix between relay j and the BS is $\boldsymbol{H}_j^r$. Although the BS also receives the noise forwarded by each relay, it was shown in [1] that the impact of such forwarded noise on the system capacity is negligible. In Section V, simulation results demonstrate that the system capacity is hardly affected by the relay noise. Therefore we only consider the additive noise at the BS.

We employ a two-stage AF relay strategy as in [4]–[8] shown in Fig. 2. In the first slot, each user transmits its signal and all relays and BS receive the signals, and the relays do not transmit. In the second slot, relays forward the signals received during the first slot and the BS receives the forward signals. The users do not transmit during the second slot.

According to the description above, by stacking the received signals by the BS in the two slots, we obtain the following signal model

$$\boldsymbol{y} = \sum_{i=1}^{K} \boldsymbol{G}_i\boldsymbol{x}_i + \boldsymbol{w}, \tag{1}$$

$$\text{with} \quad \boldsymbol{G}_i \triangleq \begin{bmatrix} \boldsymbol{H}_i\boldsymbol{F}_i \\ \sum_{j=1}^{M} \boldsymbol{H}_j^r\boldsymbol{F}_j^r\boldsymbol{H}_i^j\boldsymbol{F}_i \end{bmatrix} \tag{2}$$

where $\boldsymbol{w}$ is the additive complex Gaussian noise with zero mean and covariance matrix $\mathbb{E}\{\boldsymbol{w}\boldsymbol{w}^H\} = \frac{1}{\rho}\boldsymbol{I}$ and ρ denotes the signal-to-noise ratio (SNR). In practical systems, some of the users may not use relaying for uplink transmission because of the half-duplex penalty in rate. In that case we can simply set the relay powers for the users who choose not to employ relaying to zero. Hence the analysis developed in this paper can be applied to the general network scenario where some users employ relaying and others do not.

We assume that the MIMO channels are in general spacially correlated according to the Kronecker model [14] and can be expressed as

$$\boldsymbol{H}_i = \boldsymbol{R}_i^{\frac{1}{2}}\boldsymbol{W}_i\boldsymbol{T}_i^{\frac{1}{2}}, \tag{3}$$

$$\boldsymbol{H}_j^r = \boldsymbol{R}_j^{r\,\frac{1}{2}}\boldsymbol{W}_j^r\boldsymbol{T}_j^{r\,\frac{1}{2}}, \tag{4}$$

$$\text{and} \quad \boldsymbol{H}_i^j = \boldsymbol{R}_i^{j\,\frac{1}{2}}\boldsymbol{W}_i^j\boldsymbol{T}_i^{j\,\frac{1}{2}}. \tag{5}$$

In (3)–(5), the matrices $\boldsymbol{W}_i$, $\boldsymbol{W}_j^r$ and $\boldsymbol{W}_i^j$ contain zero-mean independent and identically distributed (i.i.d.) Gaussian entries; the matrices $\boldsymbol{R}_i, \boldsymbol{R}_j^r, \boldsymbol{R}_i^j, \boldsymbol{T}_i, \boldsymbol{T}_j^r$ and $\boldsymbol{T}_i^j$ are fixed correlation matrices. We assume that the precoding matrices $\boldsymbol{F}_i$ and $\boldsymbol{F}_j^r$ are independent of $\boldsymbol{W}_i, \boldsymbol{W}_j^r$ and $\boldsymbol{W}_i^j$. This is the case when covariance feedback is employed, i.e., when the precoders are designed based on the channel covariance matrices [15]. This assumption is also reasonable when codebook-based precoders are employed [16]–[19], e.g., the DFT codebook, in which case the correlation between the precoder and the channel is sufficiently weak. Furthermore, the path loss is taken into account in the channel model, so that different matrices have different variance profile functions [2]. In particular, we have

$$v_i \triangleq \mathrm{var}\{W_i(\cdot,\cdot)\} = (d_i)^{-\beta}, \tag{6}$$

$$v_i^j \triangleq \mathrm{var}\left\{W_i^j(\cdot,\cdot)\right\} = \left(d_i^j\right)^{-\beta}, \tag{7}$$

$$\text{and} \quad v_j^r \triangleq \mathrm{var}\left\{W_j^r(\cdot,\cdot)\right\} = \left(d_j^r\right)^{-\beta}, \tag{8}$$

where d_i denotes the distance between user i and the BS, d_i^j denotes the distance between user i and relay j, and d_j^r denotes the distance between relay j and the BS, β is the path loss exponent.

The system given by (1)–(2) is essentially a MIMO MAC model and its ergodic sum rate is given by

$$C = \mathbb{E}\left\{\log\det\left(\boldsymbol{I} + \rho\sum_{i=1}^{K}\boldsymbol{G}_i\boldsymbol{Q}_i\boldsymbol{G}_i^H\right)\right\} \tag{9}$$

where $\boldsymbol{Q}_i = \mathbb{E}\{\boldsymbol{x}_i\boldsymbol{x}_i^H\}$ is the transmit covariance matrix of user i. In general, we need to resort to Monte Carlo methods to compute the sum rate in (9). Our goal is to find some deterministic expressions that can well approximate in (9), especially for large MIMO systems and/or large number of users.

Before we move to the asymptotic and non-asymptotic analysis, we introduce the Shannon transform of the random matrix $\sum_{i=1}^{K}\boldsymbol{G}_i\boldsymbol{Q}_i\boldsymbol{G}_i^H$, given by

$$D_{N_B} = \frac{1}{2N_B}\log\det\left[\boldsymbol{I} + \rho\sum_{i=1}^{K}\boldsymbol{G}_i\boldsymbol{Q}_i\boldsymbol{G}_i^H\right], \tag{10}$$

which is simply the sum rate per receive antenna at the BS.

III. Asymptotic Analysis

In this section, we perform the asymptotic analysis and derive the deterministic equivalents for the per-receive-antenna sum rate given in (10). We consider two asymptotic cases. The first case corresponds to large MIMO dimensions but fixed number of users; whereas the second case corresponds to large MIMO dimensions and/or large number of users.

A deterministic equivalent is a deterministic approximation to some transform of a random matrix (e.g., the Shannon transform in (10)); and the approximation error goes to zero with probability one when the dimension of the random matrix goes to infinity. Specifically, suppose that $\{\boldsymbol{B}_n \in \mathbb{C}^{n\times n}\}$ is a sequence of random Hermitian matrices, and $\{f_n\}$ is a sequence of functionals of $n \times n$ matrices. A deterministic equivalent of $\boldsymbol{B}_n$ for the functional f_n is a sequence of deterministic matrices $\{\boldsymbol{B}_n^* \in \mathbb{C}^{n\times n}\}$, such that

$$\lim_{n\to\infty} f_n(\boldsymbol{B}_n) - f_n(\boldsymbol{B}_n^*) \to 0$$

with probability one. Note that $f_n(\boldsymbol{B}_n^*)$ does not need to have a limit as $n \to \infty$.

A. Large MIMO Dimensions, Fixed Number of Users

In this subsection, we derive the deterministic equivalent of the per-receive-antenna sum rate when the MIMO dimension is large but the number of users is fixed. In [3], the deterministic equivalent of the rate of a multi-hop relay system is analyzed. However, the direct link between the source and destination is ignored, whereas in this work we consider multiple two-hop relay systems with direct links.

We will make use of the results in [20] and [21] on the deterministic equivalent of the Shannon transform of a random matrix $\boldsymbol{B}_N$ of the following form:

$$\boldsymbol{B}_N = \sum_{k=1}^{K} \boldsymbol{H}_k \boldsymbol{H}_k^H, \tag{11}$$

where

$$\boldsymbol{H}_k = \left[\boldsymbol{H}_{1k}^T, \ldots, \boldsymbol{H}_{Lk}^T\right]^T, \tag{12}$$

$$\text{and} \quad \boldsymbol{H}_{lk} = \boldsymbol{R}_{lk}^{\frac{1}{2}} \boldsymbol{X}_{lk} \boldsymbol{T}_{lk}^{\frac{1}{2}}. \tag{13}$$

$\boldsymbol{X}_{lk} \in \mathbb{C}^{N\times n_k}$ has i.i.d. entries and $\frac{X_{lk}(i,j)}{\sqrt{n_k}}$ has zero mean and unit variance; $\boldsymbol{R}_{lk} \in \mathbb{C}^{N\times N}$ and $\boldsymbol{T}_{lk} \in \mathbb{C}^{n_k\times n_k}$ are non-negative definite Hermitian matrices. Under certain conditions, the deterministic equivalent of the Shannon transform of $\boldsymbol{B}_N$: $D_N(x) = \frac{1}{N}\log\det(\boldsymbol{I} + x\boldsymbol{B}_N)$ for $x > 0$ exists when N and all n_k grow large, and it depends on $\{N, n_k, \boldsymbol{R}_k, \boldsymbol{T}_k\}$ and the unique solution of a fixed point equation. In [20], the deterministic equivalent is obtained under the condition that $L = 1$ and $\boldsymbol{X}_{lk}$'s are Gaussian. This result is extended to random matrices with $L > 1$ and arbitrary distribution in [21], where it is shown that if the entries of $\boldsymbol{X}_{lk}$'s have finite 6th-order moments, then the difference between the Shannon transform of $\boldsymbol{B}_N$ in (11) and its deterministic equivalent has the order $\mathcal{O}(\frac{1}{\sqrt{N}})$. If $\boldsymbol{X}_{lk}$'s are Gaussian, the difference becomes $\mathcal{O}(\frac{1}{N})$. We have the following result.

Theorem 1: Consider the single-cell MIMO system with relays defined in Section II with one BS, K users and M relays, where the BS has N_B antennas, each user has N_U antennas and each relay has N_R antennas. Assume that the channel correlation matrices satisfy $\boldsymbol{R}_j^r \approx \boldsymbol{R}_i^r$ for $j \neq i$ and $\boldsymbol{T}_i \approx \boldsymbol{T}_i^j$. Assume further that the eigenvalues of $\boldsymbol{T}_i$ and $\boldsymbol{R}_i$ are bounded.

Define

$$\boldsymbol{S}_i^j \triangleq \boldsymbol{T}_j^{r\,\frac{1}{2}} \boldsymbol{F}_j^r \boldsymbol{R}_i^{j\,\frac{1}{2}}, \tag{14}$$

$$\text{and} \quad \boldsymbol{M}_i \triangleq \boldsymbol{T}_i^{\frac{1}{2}} \boldsymbol{F}_i \boldsymbol{Q}_i \boldsymbol{F}_i^H \boldsymbol{T}_i^{\frac{1}{2}}. \tag{15}$$

Then for fixed N_R and fixed ratio $\frac{N_B}{N_U} = a$, as $N_B \to \infty$, $N_U \to \infty$, the per-receive-antenna uplink sum rate defined in (10) satisfies

$$D_{N_B} - D_{N_B}^* \longrightarrow 0, \tag{16}$$

where the deterministic equivalent $D_{N_B}^*$ is given by

$$\begin{aligned} D_{N_B}^* = &\frac{1}{2N_B}\sum_{i=1}^{K}\log\det\left[\boldsymbol{I}_{N_U} + a\sum_{l=1}^{2} e_{l,i}\boldsymbol{M}_i\right] \\ &+ \frac{1}{2N_B}\log\det\left[\boldsymbol{I}_{N_B} + \sum_{i=1}^{K}\delta_i b_1^i \boldsymbol{R}_i\right] \\ &+ \frac{1}{2N_B}\log\det\left[\boldsymbol{I}_{N_B} + \sum_{i=1}^{K}\delta_i b_2^i \boldsymbol{R}_1^r\right] \\ &- \frac{1}{2\rho}\sum_{l,i}\delta_i e_{l,i}, \end{aligned} \tag{17}$$

where

$$b_1^i \triangleq v_i N_U, \tag{18}$$

$$\text{and} \quad b_2^i \triangleq \left(\sum_{j,k,l}\left|S_i^j(l,k)\right|^2 v_i^j v_j^r\right) N_U. \tag{19}$$

$\{e_{l,i}, \delta_i, l = 1,2, i = 1,\ldots,K\}$ form the unique solution to the following set of fixed-point equations:

$$e_{1,i} = \frac{1}{N_B}\operatorname{tr}\left[b_1^i \boldsymbol{R}_i \rho\left(\boldsymbol{I}_{N_B} + \sum_{k=1}^{K}\delta_k b_1^k \boldsymbol{R}_k\right)\right], \tag{20}$$

$$e_{2,i} = \frac{1}{N_B}\operatorname{tr}\left[b_2^i \boldsymbol{R}_1^r \rho\left(\boldsymbol{I}_{N_B} + \sum_{k=1}^{K}\delta_k b_2^k \boldsymbol{R}_1^r\right)\right], \tag{21}$$

$$\text{and} \quad \delta_i = \frac{1}{N_U}\operatorname{tr}\left[\boldsymbol{M}_i \rho\left(\boldsymbol{I}_{N_U} + a\sum_{l=1}^{2} e_{l,i}\boldsymbol{M}_i\right)^{-1}\right]. \tag{22}$$

Proof: We will transform the random matrix $\sum_{i=1}^{K}\boldsymbol{G}_i\boldsymbol{Q}_i\boldsymbol{G}_i^H$ into the form of (11) and then directly apply the result of [21] to obtain its deterministic equivalent. By using (2)–(5), we can write

$$\begin{aligned}
\sum_{i=1}^{K} \boldsymbol{G}_i\boldsymbol{Q}_i\boldsymbol{G}_i^H
&= \sum_{i=1}^{K} \begin{bmatrix} \boldsymbol{H}_i\boldsymbol{F}_i \\ \sum_{j=1}^{M} \boldsymbol{H}_j^r\boldsymbol{F}_j^r\boldsymbol{H}_i^j\boldsymbol{F}_i \end{bmatrix} \boldsymbol{Q}_i \\
&\quad \times \begin{bmatrix} \boldsymbol{H}_i\boldsymbol{F}_i \\ \sum_{j=1}^{M} \boldsymbol{H}_j^r\boldsymbol{F}_j^r\boldsymbol{H}_i^j\boldsymbol{F}_i \end{bmatrix}^H \qquad (23)\\
&= \sum_{i=1}^{K} \begin{bmatrix} \boldsymbol{R}_i^{\frac{1}{2}}\boldsymbol{W}_i \\ \boldsymbol{R}_1^{r\frac{1}{2}} \underbrace{\sum_{j=1}^{M} \boldsymbol{W}_j^r\boldsymbol{S}_i^j\boldsymbol{W}_i^j}_{\boldsymbol{\Delta}_i} \end{bmatrix} \boldsymbol{M}_i \\
&\quad \times \begin{bmatrix} \boldsymbol{R}_i^{\frac{1}{2}}\boldsymbol{W}_i \\ \boldsymbol{R}_1^{r\frac{1}{2}} \underbrace{\sum_{j=1}^{M} \boldsymbol{W}_j^r\boldsymbol{S}_i^j\boldsymbol{W}_i^j}_{\boldsymbol{\Delta}_i} \end{bmatrix}^H, \qquad (24)
\end{aligned}$$

where (24) follows from (14)–(15) and the assumption that $\boldsymbol{R}_j^r \approx \boldsymbol{R}_i^r$ for $j \neq i$ and $\boldsymbol{T}_i \approx \boldsymbol{T}_i^j$. Note that $\boldsymbol{\Delta}_i$ is an $N_B \times N_U$ random matrix with the (m,n)-th entry given by

$$\Delta_i(m,n) = \sum_{j=1}^{M}\sum_{k=1}^{N_R}\sum_{l=1}^{N_R} S_i^j(l,k)W_j^r(k,n)W_i^j(m,l). \quad (25)$$

Since the entries of $\boldsymbol{W}_i, \boldsymbol{W}_j^r$ and $\boldsymbol{W}_i^j$ are zero-mean i.i.d. Gaussian random variables, it follows that the entries of $\boldsymbol{W}_i$ and $\boldsymbol{\Delta}_i$ are i.i.d. with zero mean and variance $\frac{b_1^i}{N_U}$ and $\frac{b_2^i}{N_U}$.

Hence we have

$$\begin{aligned}
\sum_{i=1}^{K} \boldsymbol{G}_i\boldsymbol{Q}_i\boldsymbol{G}_i^H
&= \sum_{i=1}^{K} \begin{bmatrix} \sqrt{b_1^i}\boldsymbol{R}_i^{\frac{1}{2}}\frac{\boldsymbol{W}_i}{\sqrt{b_1^i}} \\ \sqrt{b_2^i}\boldsymbol{R}_1^{r\frac{1}{2}}\frac{\boldsymbol{\Delta}_i}{\sqrt{b_2^i}} \end{bmatrix} \boldsymbol{M}_i \begin{bmatrix} \sqrt{b_1^i}\boldsymbol{R}_i^{\frac{1}{2}}\frac{\boldsymbol{W}_i}{\sqrt{b_1^i}} \\ \sqrt{b_2^i}\boldsymbol{R}_1^{r\frac{1}{2}}\frac{\boldsymbol{\Delta}_i}{\sqrt{b_2^i}} \end{bmatrix}^H, \qquad (26)
\end{aligned}$$

where the entries of $\frac{\boldsymbol{W}_i}{\sqrt{b_1^i}}$ and $\frac{\boldsymbol{\Delta}_i}{\sqrt{b_2^i}}$ are i.i.d. with zero mean and variance $\frac{1}{N_U}$, which is exactly the same form as (11). Theorem 1 then follows directly from the result in [21]. ■

Given K, N_B, N_U, N_R, the channel correlation matrices $\{\boldsymbol{R}_i, \boldsymbol{R}_j^r, \boldsymbol{R}_i^j, \boldsymbol{T}_i, \boldsymbol{T}_j^r, \boldsymbol{T}_i^j\}$ and the variances $\{v_i, v_j^r, v_i^j\}$, by solving the fixed-point (20)–(22), we can then obtain the asymptotic per-receive-antenna sum rate using (17). This provides an efficient way to evaluate the system capacity since no Monte Carlo simulations are needed.

B. Large MIMO Dimensions, Large Number of Users

In the previous subsection, the number of users K is fixed and we considered the large MIMO dimension regime, i.e., $N_B \to \infty$ and $N_U \to \infty$. In this subsection, we consider another asymptotic scenario where the MIMO dimension is large and the number of users can also be large. Specifically, we let $N_B \to \infty, KN_U \to \infty$, and keep the ratio $\frac{KN_U}{N_B}$ fixed.

Our derivation of the deterministic equivalent of the asymptotic per-receive-antenna sum rate in this case is based on the following result [22], [23]. Suppose that an $N \times n$ random matrix $\boldsymbol{Z}$ whose entries are independent zero-mean random variables satisfies the Lindeberg condition

$$\frac{1}{n}\sum_{i,j} \mathbb{E}\{|Z(i,j)|^2 1\{|Z(i,j)| \geq \delta\}\} \to 0 \quad (27)$$

for any $\delta > 0$ when $N, n \to \infty$. Then the deterministic equivalent of $\boldsymbol{Z}$ and its Shannon transform for large N and n can be obtained, which is a function of the variances of the entries of $\boldsymbol{Z}$.

We focus on the random matrix in (23) and its Shannon transform D_{N_B}. Our basic idea here is to transform the matrix summation in (23) to matrix product and then explore the asymptotic characteristic of the transformed random matrix. Define

$$\boldsymbol{L}_i \triangleq \boldsymbol{T}_i^{\frac{1}{2}}\boldsymbol{F}_i\boldsymbol{Q}_i^{\frac{1}{2}}, \quad (28)$$

$$\boldsymbol{L}_i^j \triangleq \boldsymbol{T}_i^{j\frac{1}{2}}\boldsymbol{F}_i\boldsymbol{Q}_i^{\frac{1}{2}}, \quad (29)$$

$$\text{and} \quad \boldsymbol{S}_i^j \triangleq \boldsymbol{T}_j^{r\frac{1}{2}}\boldsymbol{F}_j^r\boldsymbol{R}_i^{j\frac{1}{2}}. \quad (30)$$

Then we can rewrite (23) as

$$\sum_{i=1}^{K} \boldsymbol{G}_i\boldsymbol{Q}_i\boldsymbol{G}_i^H = \boldsymbol{Z}\boldsymbol{Z}^H, \quad (31)$$

where $\boldsymbol{Z}$ is a $2N_B \times KN_U$ matrix, given by

$$\begin{aligned}
\boldsymbol{Z} &\triangleq \left[\boldsymbol{G}_1\boldsymbol{Q}_1^{\frac{1}{2}}, \ldots, \boldsymbol{G}_K\boldsymbol{Q}_K^{\frac{1}{2}}\right] \\
&= \left[\begin{matrix} \boldsymbol{R}_i^{\frac{1}{2}}\boldsymbol{W}_i\boldsymbol{L}_i \\ \sum_j \boldsymbol{R}_j^{r\frac{1}{2}}\boldsymbol{W}_j^r\boldsymbol{S}_i^j\boldsymbol{W}_i^j\boldsymbol{L}_i^j \end{matrix}, \quad i = 1, \ldots, K\right]. \quad (32)
\end{aligned}$$

Define a $2N_B \times KN_U$ matrix $\boldsymbol{\Sigma}$ whose entries are given by

$$\Sigma(s,t) \triangleq N_B \operatorname{var}\{Z(s,t)\}, \quad (33)$$

where the variance of the (s,t)-th entry of $\boldsymbol{Z}$ can be calculated as (34), shown at the bottom of the page, with $i_t = \lceil \frac{t}{N_U} \rceil - 1$ and $\lceil\cdot\rceil$ being the ceiling operator.

$$\operatorname{var}\{Z(s,t)\} = \begin{cases} \left|R_{i_t}^{\frac{1}{2}}(s,l)L_{i_t}(k, t - i_tN_U)\right|^2 v_{i_t} & \text{if } s \leq N_B \\ \sum_{j,m,n,k,l} \left|R_j^{r\frac{1}{2}}(s - N_B, l)S_{i_t}^j(m,n)L_{i_t}^j(k, t - i_tN_U)\right|^2 v_{i_t}^j v_j^r & \text{if } s > N_B \end{cases} \quad (34)$$

We have the following result.

Theorem 2: Consider the single-cell system with relays defined in Section II, where the BS has N_B antennas, each user has N_U antennas, and the cell has K users and M relays. Assume that the random matrix $\boldsymbol{Z}$ in (32) satisfies the Lindeberg condition in (27). Then by fixing the ratio $\frac{KN_U}{2N_B}=a$, and when $KN_U \to \infty, N_B \to \infty$, the per-receive-antenna sum rate D_{N_B} in (10) satisfies

$$D_{N_B} - D^*_{N_B} \longrightarrow 0, \tag{35}$$

where the deterministic equivalent $D^*_{N_B}$ is given by

$$\begin{aligned} D^*_{N_B} = & \frac{a}{KN_U}\mathbf{1}^T_{KN_U}\cdot\log[\mathbf{1}_{KN_U}+\rho\boldsymbol{\Sigma}^T\boldsymbol{u}] \\ & + \frac{1}{2N_B}\mathbf{1}^T_{2N_B}\cdot\log\left[\mathbf{1}_{2N_B}+a\rho\boldsymbol{\Sigma}\boldsymbol{v}\right] \\ & - a\rho\boldsymbol{u}^T\boldsymbol{\Sigma}\boldsymbol{v}\log e, \end{aligned} \tag{36}$$

where $\mathbf{1}_N$ denotes an N-dimensional all-1 column vector, and $\log\boldsymbol{\theta}$ denotes a column vector whose entries are the logarithms of the corresponding entries in $\boldsymbol{\theta}$. The $2N_B$-dimensional column vector $\boldsymbol{u}$ and the KN_U-dimensional column vector $\boldsymbol{v}$ form the unique solution to the following fixed-point equations

$$u_s = \frac{1}{2N_B\left(1+a\rho\sum_{t=1}^{KN_U}\Sigma(s,t)v_t\right)}, \quad s=1,\ldots,2N_B, \tag{37}$$

$$\text{and} \quad v_t = \frac{1}{KN_U(1+\rho\sum_{s=1}^{2N_B}\Sigma(s,t)u_s)}, \quad t=1,\ldots,KN_U. \tag{38}$$

Proof: See Appendix A. ■

Note that unlike Theorem 1, Theorem 2 makes no assumptions on the MIMO correlation matrices. On the other hand, the asymptotic regime of $KN_U\to\infty, N_B\to\infty$, $\frac{KN_U}{2N_B}=a$, subsumes a special case of fixed K and $N_U\to\infty$, which is the same asymptotic regime considered in Theorem 1. Numerical results in Section V indicates that with fixed K, the deterministic equivalent given by Theorem 1 is more accurate than that given by Theorem 2 when N_B and N_U are large.

IV. Non-Asymptotic Analysis

The asymptotic analysis in the previous section considers the regime of large MIMO dimensions, with the number of users either fixed or large. In this section, we consider another regime with the fixed MIMO dimensions, and large number of users. We will treat both single-cell and multi-cell cases. The tool employed for this case is the non-asymptotic analysis [24], and we will obtain deterministic upper and lower bounds which the sum rate lies in between with high probability.

Asymptotic methods explore the limiting characteristics of the eigenvalues or singular values of the random matrices. On the other hand, non-asymptotic methods try to find upper and lower bounds to constrain the singular values of the random matrices by cutting the tail of the probability distribution function (pdf) of the entries. The singular values can be constrained within the bounds with high probability because the tail of the pdf decays fast.

A. Single-Cell

In this subsection, we still focus on the random matrix $\boldsymbol{Z}$ defined in (32). Each entry of $\boldsymbol{Z}$ is the sum of Gaussian random variables and products of Gaussian random variables. It will be shown that the pdf of the entries of $\boldsymbol{Z}$ has sub-exponential decaying feature. Therefore we can obtain the bounds for the singular values of $\boldsymbol{Z}$ through cutting off the tail of the pdf of its entries.

In order to obtain the bounds on the sum rate through the bounds on the singular values of $\boldsymbol{Z}$, we rewrite the sum rate in term of the singular values:

$$\begin{aligned} C &= \mathbb{E}\{\log\det[\boldsymbol{I}+\rho\boldsymbol{Z}\boldsymbol{Z}^H]\} \\ &= \mathbb{E}\left\{\sum_{i=1}^{2N_B}\log\left[1+\rho\lambda^i_{\boldsymbol{Z}\boldsymbol{Z}^H}\right]\right\} \\ &= \mathbb{E}\left\{\sum_{i=1}^{2N_B}\log\left[1+\rho\left(s^i_{\boldsymbol{Z}}\right)^2\right]\right\}, \end{aligned} \tag{39}$$

where $\lambda^i_{\boldsymbol{Z}\boldsymbol{Z}^H}$ denotes the i-th eigenvalue of $\boldsymbol{Z}\boldsymbol{Z}^H$, and $s^i_{\boldsymbol{Z}}$ denotes the i-th singular value of $\boldsymbol{Z}$.

Note that from (32), we can write

$$\boldsymbol{Z} = \begin{bmatrix}\boldsymbol{Z}_G\\ \boldsymbol{Z}_E\end{bmatrix} = \begin{bmatrix}\boldsymbol{Z}^1_G, & \ldots, & \boldsymbol{Z}^K_G\\ \boldsymbol{Z}^1_E, & \ldots, & \boldsymbol{Z}^K_E\end{bmatrix}, \tag{40}$$

where

$$\boldsymbol{Z}^i_G \triangleq \boldsymbol{R}_i^{\frac{1}{2}}\boldsymbol{W}_i\boldsymbol{L}_i, \tag{41}$$

$$\text{and} \quad \boldsymbol{Z}^i_E \triangleq \sum_{j=1}^{M}\boldsymbol{R}^{r\,\frac{1}{2}}_j\boldsymbol{W}^r_j\boldsymbol{S}^j_i\boldsymbol{W}^j_i\boldsymbol{L}^j_i. \tag{42}$$

Then similar to (34), we have (43) and (44),

$$\operatorname{var}\{Z_G(s,t)\} = \sum_{h,l}\left|R^{\frac{1}{2}}_{i_t}(s,l)L_{i_t}(h,t-i_tN_U)\right|^2 v_{i_t}, \tag{43}$$

$$\text{and} \quad \operatorname{var}\{Z_E(s,t)\} = \sum_{j,m,n,h,l}\left|R^{r\,\frac{1}{2}}_j(s,l)S^j_{i_t}(m,n)L^j_{i_t}(h,t-i_tN_U)\right|^2 v^j_{i_t}v^r_j, \tag{44}$$

where $i_t = \lceil\frac{t}{N_U}\rceil - 1$

We have the following result on the sum rate bounds for fixed MIMO dimensions and large number of users.

Theorem 3: Consider the single-cell system with relays defined in Section II, where the BS has N_B antennas, each user has N_U antennas, and the cell has K users and M relays. For any $q>0$ and large K, with probability at least

$$1-2[\exp(-c_1\sqrt{KN_U}q)+\exp(-c_2q^2)], \tag{45}$$

we have

$$\begin{aligned} &\sqrt{2KN_U}-2c_3\sqrt{N_B}-\sqrt{2}q \le s_{\boldsymbol{Z}} \\ &\le \sqrt{2KN_U}+2c_3\sqrt{N_B}+\sqrt{2}q. \end{aligned} \tag{46}$$

If we choose q to ensure the lower bound in (46) is positive, we then have with probability in (45)

$$\begin{aligned}&2N_B\log[1+\rho(\sqrt{2KN_U}-2c_3\sqrt{N_B}-\sqrt{2}q)^2]\\&\le C\\&\le 2N_B\log[1+\rho(\sqrt{2KN_U}+2c_3\sqrt{N_B}+\sqrt{2}q)^2],\end{aligned} \tag{47}$$

where c_1, c_2 and c_3 are constants satisfying (48)–(50).

Proof: See Appendix B. ■

The valid ranges of the constants c_1, c_2 and c_3 are given as follows based on Appendix B:

$$\frac{8N_B\log 9}{KN_U}\le c_1\le K\max\left(\frac{1}{K_E},\frac{1}{K_E^2}\right) \tag{48}$$

$$\frac{8N_B\log 9}{KN_U}\le c_2\le K\max\left(\frac{1}{K_G^4},\frac{1}{K_G^2}\right) \tag{49}$$

$$\text{and}\quad 2\max\left(\sqrt{\frac{\log 9}{c_2}},2\sqrt{\frac{2N_B}{KN_U}\frac{\log 9}{c_1}}\right)\le c_3\le\sqrt{\frac{KN_U}{2N_B}}, \tag{50}$$

where

$$K_G\triangleq\max_k(2e^3\mathrm{var}^2\{Z_G(1,k)\}), \tag{51}$$

$$\text{and}\quad K_E\triangleq\max_k(e^2\sqrt{2\mathrm{var}\{Z_E(1,k)\}}). \tag{52}$$

Since we would like to make the bounds tight and maximize the probability that the sum rate C lies within the bounds, we choose the parameters as follows:

$$c_1=K\max\left(\frac{1}{K_E},\frac{1}{K_E^2}\right), \tag{53}$$

$$c_2=K\max\left(\frac{1}{K_G^4},\frac{1}{K_G^2}\right), \tag{54}$$

$$\text{and}\quad c_3=2\max\left(\sqrt{\frac{\log 9}{c_2}},2\sqrt{\frac{2N_B}{KN_U}\frac{\log 9}{c_1}}\right). \tag{55}$$

Moreover from (45) and (47), when q is large, the probability that C is between the bounds is large, but the gap between the bounds is also large.

If we use B_U and B_L to denote the upper and lower bounds in Theorem 3, respectively, then the gap between the upper and lower bounds satisfies the following

$$\begin{aligned}&\lim_{K\to\infty}(B_U-B_L)\\&=2N_B\lim_{K\to\infty}\log\frac{1+\rho(\sqrt{2KN_U}+2c_3\sqrt{N_B}+\sqrt{2}q)^2}{1+\rho(\sqrt{2KN_U}-2c_3\sqrt{N_B}-\sqrt{2}q)^2}\\&=0.\end{aligned} \tag{56}$$

The bounds are asymptotically tight from this point of view. Furthermore, if we choose the parameters according to (53)–(55), then $c_1, c_2\to\infty$ as $K\to\infty$ since the variances do not change with K. Therefore the probability in (45) tends to 1 as $K\to\infty$.

Compared with the asymptotic results in the previous section, the non-asymptotic bounds can be used for regular MIMO systems with small numbers of transmit and receive antennas. Moreover, the non-asymptotic bounds are even simpler to compute than the asymptotic results since they do not involve solving fixed-point equations. Note that although the bounds in (47) are expressed in terms of K, N_B, N_U and ρ, the constants c_1, c_2 and c_3 are functions of N_R as well as the correlation matrices.

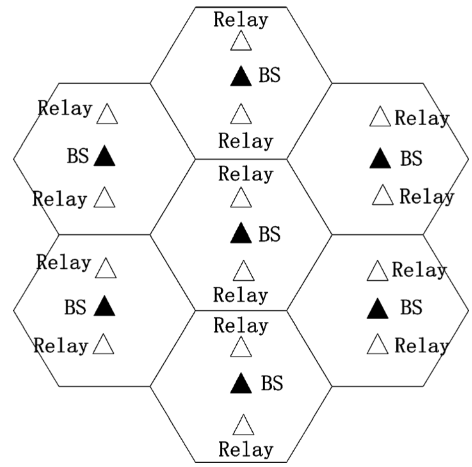

Fig. 3. A multi-cell MIMO system with relays.

B. Multi-Cell

We next extend the result obtained from the previous subsection for single cell to the multi-cell case, where the base stations jointly process the received signals to mitigate the effect of inter-cell interference.

The multi-cell system is depicted in Fig. 3, where there are totally N_C BSs, M relays, and K users. As in the single-cell case, the relays receive signals from users and forward them to the BSs. Each BS receives signals from all users and relays.

We denote $\boldsymbol{x}_i$ as the transmitted signal from user i and $\boldsymbol{y}_n$ as the signal received by BS n. The numbers of antennas at each BS, relay and user are N_B, N_R and N_U, respectively. The channel matrices between user i and BS n, between user i and relay j and between relay j and BS n are denotes as $\boldsymbol{H}_i^n, \bar{\boldsymbol{H}}_i^j$ and $\tilde{\boldsymbol{H}}_j^n$, respectively. Moreover the precoding matrices of user i and relay j are denoted as $\boldsymbol{F}_i$ and $\boldsymbol{F}_j^r$, respectively. As before, unit transmit power is assumed, i.e., $\mathbb{E}\{\boldsymbol{x}_i^H\boldsymbol{x}_i\}=1$.

By stacking the received signals at all BSs in two time slots, we have the following multi-cell uplink signal model

$$\boldsymbol{y}=\begin{bmatrix}\boldsymbol{G}_1^1 & \cdots & \boldsymbol{G}_1^K\\ \vdots & \ddots & \vdots\\ \boldsymbol{G}_{N_C}^1 & \cdots & \boldsymbol{G}_{N_C}^K\\ \tilde{\boldsymbol{G}}_1^1 & \cdots & \tilde{\boldsymbol{G}}_1^K\\ \vdots & \ddots & \vdots\\ \tilde{\boldsymbol{G}}_{N_C}^1 & \cdots & \tilde{\boldsymbol{G}}_{N_C}^K\end{bmatrix}\begin{bmatrix}\boldsymbol{x}_1\\ \vdots\\ \boldsymbol{x}_K\end{bmatrix}+\boldsymbol{w}, \tag{57}$$

where

$$\boldsymbol{G}_i^n\triangleq\boldsymbol{H}_i^n\boldsymbol{F}_i, \tag{58}$$

$$\text{and}\quad \tilde{\boldsymbol{G}}_i^n\triangleq\sum_{j=1}^{M}\tilde{\boldsymbol{H}}_j^n\boldsymbol{F}_j^r\bar{\boldsymbol{H}}_i^j\boldsymbol{F}_i. \tag{59}$$

$\boldsymbol{w}$ is the $2N_C N_B \times 1$ additive complex Gaussian noise vector with covariance matrix $\mathbb{E}\{\boldsymbol{w}\boldsymbol{w}^H\} = \frac{1}{\rho}\boldsymbol{I}$, where ρ denotes the SNR.

Under the Kronecker model, the channels are expressed as

$$\boldsymbol{H}_i^n = \boldsymbol{R}_i^{n\frac{1}{2}} \boldsymbol{W}_i^n \boldsymbol{T}_i^{n\frac{1}{2}}, \tag{60}$$

$$\tilde{\boldsymbol{H}}_j^n = \tilde{\boldsymbol{R}}_j^{n\frac{1}{2}} \tilde{\boldsymbol{W}}_j^n \tilde{\boldsymbol{T}}_j^{n\frac{1}{2}}, \tag{61}$$

$$\text{and} \quad \bar{\boldsymbol{H}}_i^j = \bar{\boldsymbol{R}}_i^{j\frac{1}{2}} \bar{\boldsymbol{W}}_i^j \bar{\boldsymbol{T}}_i^{j\frac{1}{2}}, \tag{62}$$

where $\boldsymbol{R}_i^n$, $\tilde{\boldsymbol{R}}_j^n$ and $\bar{\boldsymbol{R}}_i^j$ are receive antenna correlation matrices, $\boldsymbol{T}_i^n$, $\tilde{\boldsymbol{T}}_j^n$ and $\bar{\boldsymbol{T}}_i^j$ are transmit antenna correlation matrices, and $\boldsymbol{W}_i^n$, $\tilde{\boldsymbol{W}}_j^n$ and $\bar{\boldsymbol{W}}_i^j$ are zero-mean i.i.d. Gaussian matrices. Furthermore, considering path loss, the variances of the entries of Gaussian matrices are

$$v_i^n \triangleq \mathrm{var}\left\{W_i^n(\cdot,\cdot)\right\} = (d_i^n)^{-\beta}, \tag{63}$$

$$\bar{v}_i^j \triangleq \mathrm{var}\left\{\bar{W}_i^j(\cdot,\cdot)\right\} = \left(\bar{d}_i^j\right)^{-\beta}, \tag{64}$$

$$\text{and} \quad \tilde{v}_j^n \triangleq \mathrm{var}\left\{\tilde{W}_j^n(\cdot,\cdot)\right\} = \left(\tilde{d}_j^n\right)^{-\beta}, \tag{65}$$

where β is the path loss exponent, d_i^n is the distance between user i and BS n, $\bar{d}_i^j$ is the distance between user i and relay j and $\tilde{d}_j^n$ is the distance between relay j and BS n.

Denote $\boldsymbol{G}_i \triangleq [\boldsymbol{G}_i^{1T}, \ldots, \boldsymbol{G}_i^{N_C T}, \tilde{\boldsymbol{G}}_i^{1T}, \ldots, \tilde{\boldsymbol{G}}_i^{N_C T}]^T$. The per-cell sum rate is then

$$\begin{aligned} C &= \mathbb{E}\left[\frac{1}{N_C}\log\det\left(\boldsymbol{I} + \rho\sum_{i=1}^{K}\boldsymbol{G}_i\boldsymbol{Q}_i\boldsymbol{G}_i^H\right)\right] \\ &= \mathbb{E}\left[\frac{1}{N_C}\log\det(\boldsymbol{I} + \rho\boldsymbol{Z}\boldsymbol{Z}^H)\right], \end{aligned} \tag{66}$$

where $\boldsymbol{Q}_i = \mathbb{E}\{\boldsymbol{x}_i\boldsymbol{x}_i^H\}$ is the transmit covariance matrix of user i, and $\boldsymbol{Z} \triangleq [\boldsymbol{G}_1\boldsymbol{Q}_1^{\frac{1}{2}}, \ldots, \boldsymbol{G}_K\boldsymbol{Q}_K^{\frac{1}{2}}]$.

Denote

$$\boldsymbol{Z}_G^{i,n} \triangleq \boldsymbol{H}_i^n \boldsymbol{F}_i \boldsymbol{Q}_i^{\frac{1}{2}}, \tag{67}$$

$$\boldsymbol{Z}_E^{i,n} \triangleq \sum_{j=1}^{M} \tilde{\boldsymbol{H}}_j^n \boldsymbol{F}_j^r \bar{\boldsymbol{H}}_i^j \boldsymbol{F}_i \boldsymbol{Q}_i^{\frac{1}{2}}, \tag{68}$$

$$\boldsymbol{Z}_G \triangleq \begin{bmatrix} \boldsymbol{Z}_G^{1,1} & \ldots & \boldsymbol{Z}_G^{K,1} \\ \vdots & \ddots & \vdots \\ \boldsymbol{Z}_G^{1,N_C} & \ldots & \boldsymbol{Z}_G^{K,N_C} \end{bmatrix}, \tag{69}$$

$$\text{and} \quad \boldsymbol{Z}_E \triangleq \begin{bmatrix} \boldsymbol{Z}_E^{1,1} & \ldots & \boldsymbol{Z}_E^{K,1} \\ \vdots & \ddots & \vdots \\ \boldsymbol{Z}_E^{1,N_C} & \ldots & \boldsymbol{Z}_E^{K,N_C} \end{bmatrix}. \tag{70}$$

Then we have

$$\boldsymbol{Z} = \begin{bmatrix} \boldsymbol{Z}_G \\ \boldsymbol{Z}_E \end{bmatrix}. \tag{71}$$

Furthermore, if we define

$$\boldsymbol{L}_i^n \triangleq \boldsymbol{T}_i^{n\frac{1}{2}} \boldsymbol{F}_i \boldsymbol{Q}_i^{\frac{1}{2}}, \tag{72}$$

$$\bar{\boldsymbol{L}}_i^j \triangleq \bar{\boldsymbol{T}}_i^{j\frac{1}{2}} \boldsymbol{F}_i \boldsymbol{Q}_i^{\frac{1}{2}}, \tag{73}$$

$$\text{and} \quad \boldsymbol{S}_i^{j,n} \triangleq \tilde{\boldsymbol{T}}_j^{n\frac{1}{2}} \boldsymbol{F}_j^r \bar{\boldsymbol{R}}_i^{j\frac{1}{2}}, \tag{74}$$

then we have (75) and (76),

$$\begin{aligned} &\mathrm{var}\{Z_G(s,k)\} \\ &\quad = \sum_{l,t}\left|R_{i_k}^{n_s\frac{1}{2}}(s - n_s N_B, l) L_{i_k}^{n_s}(t, k - i_k N_U)\right|^2 v_{i_k}^{n_s}, \end{aligned} \tag{75}$$

$$\begin{aligned} \text{and} \quad &\mathrm{var}\{Z_E(s,k)\} \\ &= \sum_{j,l,m,h,t}\left|\tilde{R}_j^{n_s\frac{1}{2}}(s - n_s N_B, l) S_{i_k}^{j,n_s}(m,h)\right. \\ &\quad \left.\times \bar{L}_{i_k}^j(t, k - i_k N_U)\right|^2 \bar{v}_{i_k}^j \tilde{v}_j^{n_s}, \end{aligned} \tag{76}$$

where $i_k = \lceil \frac{k}{N_U} \rceil - 1$ and $n_s = \lceil \frac{s}{N_B} \rceil - 1$.

We now extend the non-asymptotic single-cell sum rate bounds in Theorem 3 to the bounds on the multi-cell per-cell sum rate.

Corollary 1: Consider a multi-cell system with relays described above, where there are N_C BSs, M relays and K users. Each BS has N_B antennas and each user has N_U antennas. For any $q > 0$ and large K, with the probability at least

$$1 - 2[\exp(-c_1\sqrt{KN_U}q) + \exp(-c_2 q^2)], \tag{77}$$

the singular values of the random matrix $\boldsymbol{Z}^H$ satisfy

$$\begin{aligned} &\sqrt{2KN_U} - 2c_3\sqrt{N_C N_B} - \sqrt{2}q \\ &\qquad \le s_{\boldsymbol{Z}} \le \sqrt{2KN_U} + 2c_3\sqrt{N_C N_B} + \sqrt{2}q. \end{aligned} \tag{78}$$

If we choose q to ensure the lower bound in (78) is positive, then for the per-cell sum rate C we have with probability in (77)

$$\begin{aligned} &2N_B\log[1 + \rho(\sqrt{2KN_U} - 2c_3\sqrt{N_C N_B} - \sqrt{2}q)^2] \\ &\quad \le C \\ &\quad \le 2N_B\log[1 + \rho(\sqrt{2KN_U} + 2c_3\sqrt{N_C N_B} + \sqrt{2}q)^2], \end{aligned} \tag{79}$$

where c_1, c_2 and c_3 are constants satisfying (80)–(82).

Similar to (53)–(55), we set the constants as:

$$c_1 = K\max\left(\frac{1}{K_E}, \frac{1}{K_E^2}\right), \tag{80}$$

$$c_2 = K\max\left(\frac{1}{K_G^4}, \frac{1}{K_G^2}\right), \tag{81}$$

$$\text{and} \quad c_3 = 2\max\left(\sqrt{\frac{\log 9}{c_2}}, 2\sqrt{\frac{2N_C N_B}{KN_U}\frac{\log 9}{c_1}}\right) \tag{82}$$

where

$$K_G \triangleq \max_{k,s}(2e^3\mathrm{var}^2\{Z_G(s,k)\}), \tag{83}$$

$$\text{and} \quad K_E \triangleq \max_{k,s}(e^2\sqrt{2\mathrm{var}\{Z_E(s,k)\}}). \tag{84}$$

Similar to (56), the bounds become tight with probability one as $K \to \infty$.

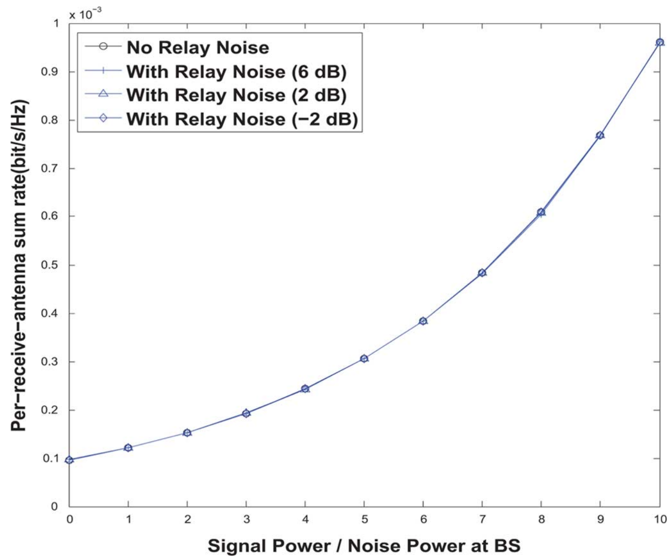

Fig. 4. The impact of relay noise on the per-receive-antenna sum rate.

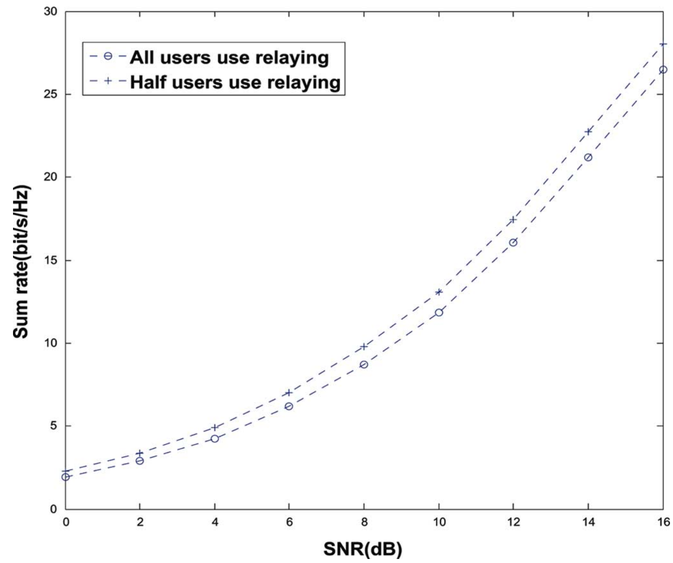

Fig. 5. Sum rates for two scenarios of relaying.

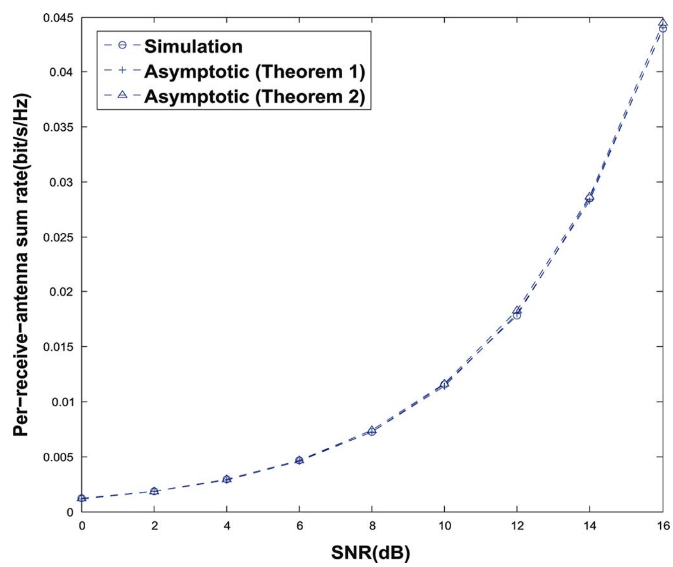

Fig. 6. Per-receive-antenna sum rate as a function of SNR.

V. Numerical Results

In this section, we illustrate the accuracy of the asymptotic and non-asymptotic rate expressions derived in the previous sections, by comparing them with simulation results. In all simulations, the radius of each cell is 10 meters. Moreover, for the variance profiles in (7)–(8) and (64)–(65), we set $\beta = 4$. The correlation matrices have the form of $\boldsymbol{UDU}^H$, where $\boldsymbol{U}$ is a random unitary matrix [25], and $\boldsymbol{D}$ is a diagonal matrix with positive entries. The DFT precoders [26], [27] are employed by the users and relays, and the codebook contains 4 DFT matrices.

A. Asymptotic Results

For the single-cell case, the BS is located at the center of the cell. Relays are placed uniformly on a circle centered at the BS with a radius of 5 meters, and users are located randomly in the cell. The distances between users and the BS and the distances between users and relays are computed based on their positions.

In order to show how performance is affected by the relay noise, we conduct a simulation on per-receive-antenna sum rate with and without relay noise. We set the number of relays $M = 1$, the number of antennas at each relay $N_R = 8$ and the number of users $K = 1$. The numbers of antennas at each user and at the BS are $N_U = 8$ and $N_B = 32$. Signal power is set as 0 dB. The relay noise power we evaluate is -2 dB, 2 dB and 6 dB. Fig. 4 verifies that the impact of relay noise on the sum rate is sufficiently small to be ignored.

In Fig. 5, we compare the the sum rates of two network scenarios: one is that all users employ relaying, and the other is that only half of the users employ relaying with the corresponding relay powers added to the transmission powers to make a fair comparison. In this simulation, we set $K = 4, N_U = 8, N_B = 32, M = 8$ and $N_R = 8$. It is seen that because of the relays' half-duplex penalty, the sum rate for the case that all users choose to use relaying is slightly lower than that for the other case.

Fig. 6 shows the per-receive-antenna sum rate obtained by simulations and the deterministic equivalents given by Theorems 1 and 2. We set $M = 8$ and $N_R = 8$. We consider the scenario that $K = 4, N_U = 8$ and $N_B = 32$. It is seen from Fig. 6 that both theorems provide fairly accurate deterministic approximations to the per-receive-antenna sum rate.

In Fig. 7, we show the convergence of the two theorems with the increasing MIMO dimensions. We set $K = 4$ and $N_B = 32$. Moreover we set $M = 8, N_R = 8$ and $\mathrm{SNR} = 8$ dB. The per-receive-antenna sum rate is shown as a function of N_U in Fig. 7. It is seen that as the MIMO dimension grows, the deterministic equivalents given by Theorems 1 and 2 converge to the true rate.

Fig. 8 illustrates the per-receive-antenna sum rate as a function of the number of relays M. We set $K = 4, N_U = 8, N_B = 32, N_R = 8$, and $\mathrm{SNR} = 8\mathrm{dB}$. It is seen that both deterministic equivalents provide good approximations to the true rate. Moreover, the rate increases as the number of relays increases, although the rate of the increase is quite slow.

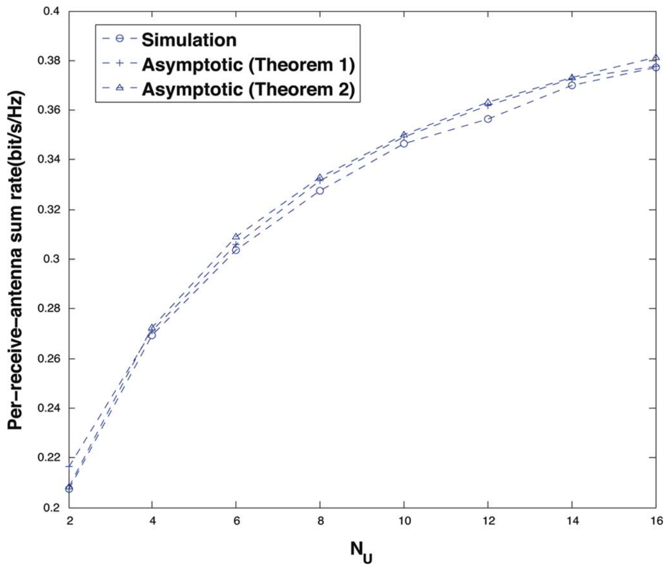

Fig. 7. Per-receive-antenna sum rate as a function of N_U.

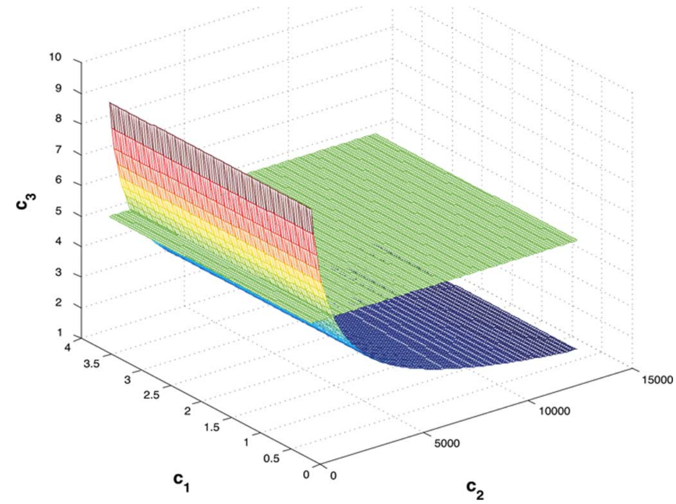

Fig. 9. The range of c_1, c_2 and c_3 specified by (48)–(50).

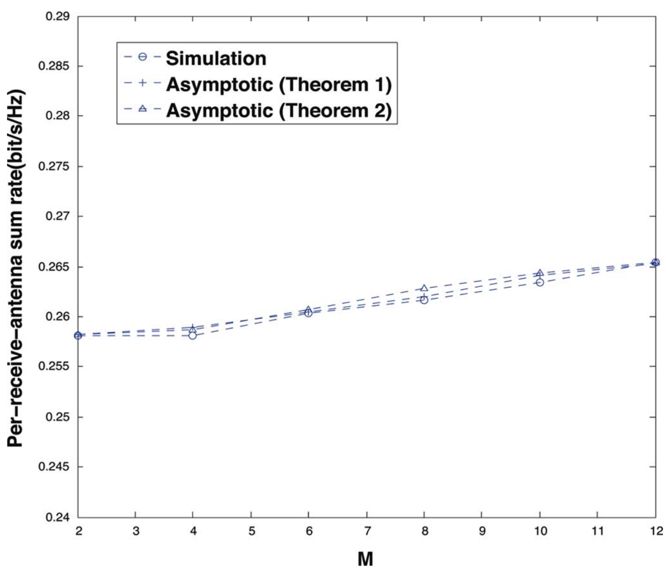

Fig. 8. Per-receive-antenna sum rate as a function of the number of relays M.

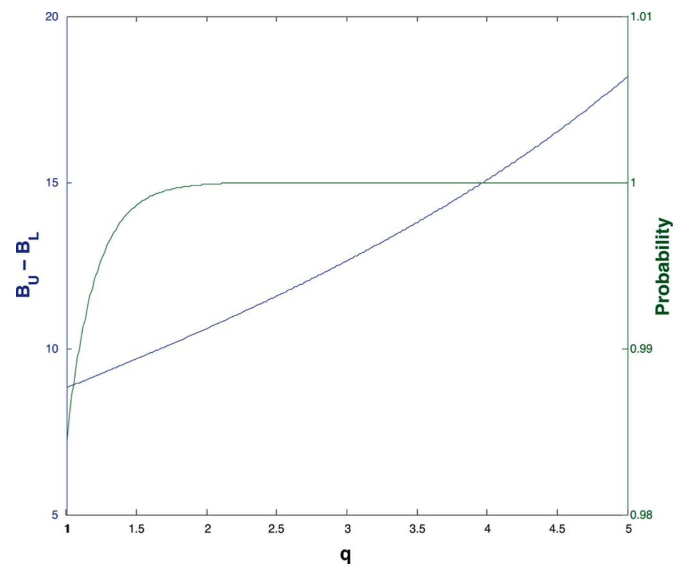

Fig. 10. The bound gap $B_U - B_L$ and the probability in (45) as a function of q.

B. Non-Asymptotic Results

For non-asymptotic analysis, we consider both single-cell and multi-cell cases. The single-cell setup is the same as before. The multi-cell setup is shown in Fig. 3, where there are $N_C = 7$ hexagonal cells with a BS at the center of each cell. The cell radius is 10 meters and in each cell the relays are located on a circle that is 5 meters from the BS. The users are randomly located in different cells.

In Fig. 9 we plot the ranges of the constants c_1, c_2 and c_3 according to (48)–(50) for a single-cell system. The number of users in the cell is $K = 40$ and the number of relays in a cell is $M = 8$. Moreover, $N_R = 8$ and $N_U = N_B = 4$. The space above the curvy plane and below the flat plane is the region for the constants. If we choose c_1, c_2 and c_3 according to (53)–(55), in Fig. 10, we plot the bound gap $B_U - B_L$ and the probability in (45) as a function of q. It is seen that as q increases, the probability also increases, but the gap between the upper and lower bounds becomes larger.

In Fig. 11 we plot the upper and lower bounds on the sum rate of a single-cell system with the corresponding probabilities. We set $M = 8, N_R = 8$, and $N_U = N_B = 4$. According to Fig. 9 and Section IV, we set $q = 1$ and choose c_1, c_2 and c_3 according to (53)–(55). The bounds corresponding to $K = 40$ and $K = 60$ are plotted in Fig. 11. In Fig. 12, with the same setup as that in Fig. 11 and $\mathrm{SNR} = 8$ dB, we plot the convergence of the gap between the upper and lower bounds as a function of K. It is seen that as K increases, the gap becomes smaller, i.e., the bounds become tighter.

Finally, the per-cell sum rate performance for a multi-cell system is shown in Fig. 13. The system parameters for each cell are the same as those for Fig. 11. Comparing Figs. 11 and 13 it is observed that the upper bound of the single-cell sum rate is smaller than the lower bound of the multi-cell per cell sum rate with the same number of users per cell. Hence by employing joint processing in multi-cell systems, the per-cell sum rate can be made larger than that in a single-cell system.

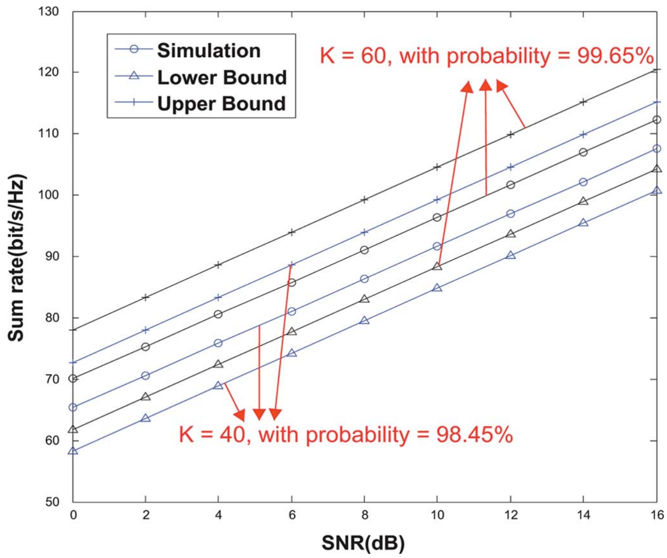

Fig. 11. Upper and lower bounds on sum rate in a single-cell system as a function of SNR.

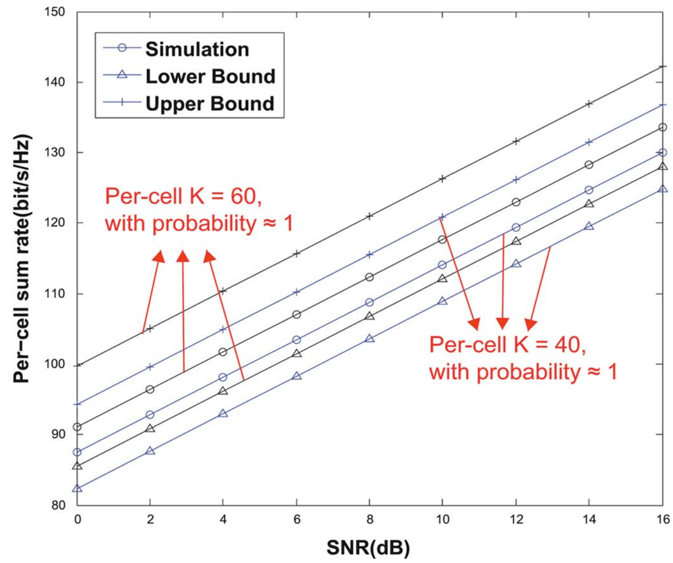

Fig. 13. Upper and lower bounds on per-cell sum rate in a multi-cell system as a function of SNR.

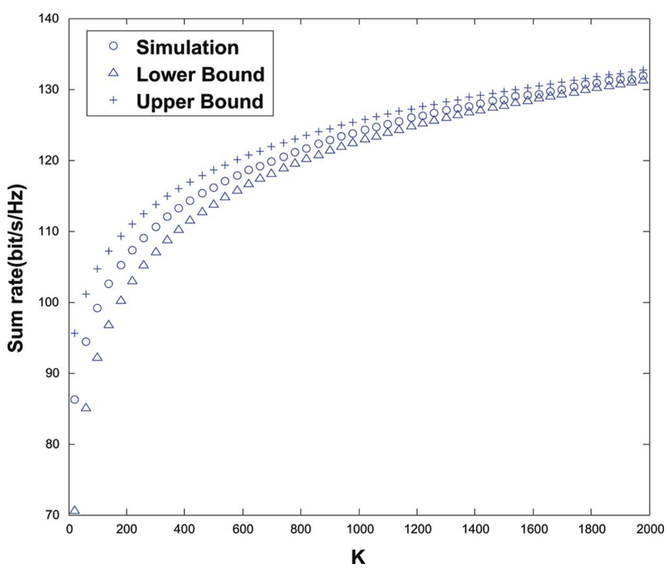

Fig. 12. Upper and lower bounds on sum rate in a single-cell system as a function of the number of users K.

VI. Conclusion

We have considered MIMO cellular networks with multiple relay stations deployed in each cell that help relay user signals to the base stations by using the amplify-and-forward strategy. We have obtained several deterministic expressions for the uplink ergodic sum rate of such systems. In particular, using the random matrix analysis tool, we have obtained two deterministic sum rate expressions for the case of large MIMO dimensions, with fixed or large number of users, respectively. And by using the non-asymptotic analysis tool, we have obtained tight upper and lower bounds on the sum rate for the case of arbitrary MIMO dimensions and large number of users. These deterministic sum rate expressions can be evaluated given the system parameters such as the numbers of relays, users, base stations, the numbers of antennas at the user, relay, and base station, the locations of the users and relays, the transmit precoding schemes employed, as well as the MIMO channel correlation statistics. With these analytical expressions, we can evaluate the sum rate of a single-cell or multi-cell network without resorting to Monte Carlo simulations. Therefore they can be useful tools for the design and analysis of relay-assisted MIMO cellular networks.

Appendix A
Proof of Theorem 2

In order to use the results in [22] and [23], we first transform the entries of the $2N_B \times KN_U$ matrix $\mathbf{\Sigma}$ in (33) into a two-dimensional function $p_\Sigma : [0,1)^2 \to \mathbb{R}$ defined as

$$p_\Sigma(x,y) = \Sigma(s,t), \tag{85}$$

if $\frac{s-1}{2N_B} \le x < \frac{s}{2N_B}$ and $\frac{t-1}{KN_U} \le y < \frac{t}{KN_U}$. Then, according to [22], [23], if $\boldsymbol{Z}$ satisfies the Lindeberg condition in (27), we have $D_{N_B} \longrightarrow D^*_{N_B}$ with

$$\begin{aligned} D^*_{N_B} = a \int_0^1 \log\left[1 + \rho \int_0^1 p_\Sigma(x,y)U(x)dx\right] dy \\ + \int_0^1 \log\left[1 + a\rho \int_0^1 p_\Sigma(x,y)V(y)dy\right] dx \\ - a\rho \int\int_{[0,1)^2} p_\Sigma(x,y)U(x)V(y)dxdy \log e, \end{aligned} \tag{86}$$

where $U(x)$ and $V(y)$ form the unique solution to the following fixed-point equations

$$U(x) = \frac{1}{1 + a\rho \int_0^1 p_\Sigma(x,y)V(y)dy}, \tag{87}$$

$$\text{and} \quad V(y) = \frac{1}{1 + \rho \int_0^1 p_\Sigma(x,y)U(x)dx}. \tag{88}$$

We next express $D^*_{N_B}$ in terms of $\mathbf{\Sigma}$.

Using the definition of $p_\Sigma(x,y)$, we have

$$\begin{aligned}
D^*_{N_B} &= \frac{a}{KN_U}\sum_{t=1}^{KN_U}\log\left[1+\rho\sum_{s=1}^{2N_B}\Sigma(s,t)\int_{\frac{s-1}{2N_B}}^{\frac{s}{2N_B}}U(x)dx\right]\\
&\quad+\frac{1}{2N_B}\sum_{s=1}^{2N_B}\log\left[1+a\rho\sum_{t=1}^{KN_U}\Sigma(s,t)\int_{\frac{t-1}{KN_U}}^{\frac{t}{KN_U}}V(y)dy\right]\\
&\quad-a\rho\sum_{t=1}^{KN_U}\sum_{s=1}^{2N_B}\Sigma(s,t)\int_{\frac{s-1}{2N_B}}^{\frac{s}{2N_B}}U(x)dx\\
&\times\int_{\frac{t-1}{KN_U}}^{\frac{t}{KN_U}}V(y)dy\log e. \qquad (89)
\end{aligned}$$

Similarly we write (87)–(88) in terms of $\boldsymbol{\Sigma}$:

$$U(x)=\frac{1}{1+a\rho\sum_{t=1}^{KN_U}\Sigma(s,t)\int_{\frac{t-1}{KN_U}}^{\frac{t}{KN_U}}V(y)dy}, \qquad (90)$$

$$\text{and}\quad V(y)=\frac{1}{1+\rho\sum_{s=1}^{2N_B}\Sigma(s,t)\int_{\frac{s-1}{2N_B}}^{\frac{s}{2N_B}}U(x)dx}. \qquad (91)$$

If we define

$$u_s\triangleq\int_{\frac{s-1}{2N_B}}^{\frac{s}{2N_B}}U(x)dx, \qquad (92)$$

$$\text{and}\quad v_t\triangleq\int_{\frac{t-1}{KN_U}}^{\frac{t}{KN_U}}V(y)dy, \qquad (93)$$

and substitute them into (89), we obtain (36). Furthermore, if we integrate over x from $\frac{s-1}{2N_B}$ to $\frac{s}{2N_B}$ on both sides of (90) and integrate over y from $\frac{t-1}{KN_U}$ to $\frac{t}{KN_U}$ on both sides of (91), and use (92)–(93), then (90) and (91) can be transformed into (37) and (38). Therefore Theorem 2 is proved.

Appendix B
Proof of Theorem 3

The proof starts from the following lemma [24]

Lemma 1: If a matrix $\boldsymbol{B}$ satisfies

$$\|\boldsymbol{B}\boldsymbol{B}^H-\boldsymbol{I}\|\le\max(\delta,\delta^2), \qquad (94)$$

for some $\delta>0$, where $\|\cdot\|$ denotes the operator norm of a matrix, then

$$1-\delta\le s^{\min}_{\boldsymbol{B}}\le s^{\max}_{\boldsymbol{B}}\le 1+\delta. \qquad (95)$$

Setting $\boldsymbol{B}=\frac{\boldsymbol{Z}^H}{\sqrt{2KN_U}}$, our goal is to find some δ and calculate the probability

$$\mathrm{P}\{\|\boldsymbol{B}\boldsymbol{B}^H-\boldsymbol{I}\|\ge\max(\delta,\delta^2)\}. \qquad (96)$$

Then we can find the bounds on the singular values of $\boldsymbol{Z}$ as well as the probability that the singular values are constrained within the bounds. In order to obtain this probability, we need to explore the distributions of the entries of $\boldsymbol{Z}_G$ and $\boldsymbol{Z}_E$ in (40).

We define $\boldsymbol{A}\triangleq\boldsymbol{Z}^H=[\boldsymbol{A}_G\ \boldsymbol{A}_E]$, where $\boldsymbol{A}_G\triangleq\boldsymbol{Z}_G^H$ and $\boldsymbol{A}_E\triangleq\boldsymbol{Z}_E^H$. It is obvious from (42) that the entries of $\boldsymbol{Z}_G^i$ are independent Gaussian random variables. The following lemma characterizes the distribution of the entries of $\boldsymbol{Z}_E^i$ in (42)

Lemma 2: The product of two independent zero-mean Gaussian random variables is a sub-exponential random variable.

Proof: Assume $W=W_1W_2$, where W_1 and W_2 are independent zero-mean Gaussian random variables with variances v_1 and v_2 respectively, so $\mathrm{var}\{W\}=v_1v_2$. Thus we have for any $q>0$

$$\begin{aligned}
&\mathrm{P}\{|\,W_1W_2\,|\ge q\}\\
&=2\mathrm{P}\{W_1W_2\ge q\}\\
&=4\mathrm{P}\left\{W_2\ge\frac{q}{W_1},W_1>0\right\}\\
&=4\int_0^\infty Q\left(\frac{q}{\sqrt{v_2}W_1}\right)\frac{1}{\sqrt{2\pi v_1}}\exp\left(-\frac{W_1^2}{2v_1}\right)dW_1\\
&\le 4\int_0^\infty\frac{1}{\sqrt{2\pi v_1}}\exp\left[-\left(\frac{\frac{q^2}{2v_2}}{W_1^2}+\frac{W_1^2}{2v_1}\right)\right]dW_1\\
&=2\exp\left(-\frac{q}{\sqrt{v_1v_2}}\right)\\
&\le\exp\left(1-\frac{q}{\sqrt{\mathrm{var}\{W\}}}\right). \qquad (97)
\end{aligned}$$

According to the definition of sub-exponential random variables in [24], we obtain Lemma 2. ■

By Lemma 2, the entries of $\boldsymbol{Z}_E^i$ in (42) are linear combinations of sub-exponential random variables. Then we can bound the probability in (96) by exploring the decaying feature of the pdfs of $\boldsymbol{Z}_E^i$ and $\boldsymbol{Z}_G^i$.

We have

$$\begin{aligned}
\|\boldsymbol{B}\boldsymbol{B}^H-\boldsymbol{I}\|&=\|\frac{1}{2KN_U}\left(\boldsymbol{A}_G\boldsymbol{A}_G^H+\boldsymbol{A}_E\boldsymbol{A}_E^H\right)-\boldsymbol{I}\|\\
&\le\frac{1}{2}\left\|\frac{1}{KN_U}\boldsymbol{A}_G\boldsymbol{A}_G^H\right\|+\frac{1}{2}\left\|\frac{1}{KN_U}\boldsymbol{A}_E\boldsymbol{A}_E^H\right\|\\
&\le\max_{\boldsymbol{x},\boldsymbol{y}\in\mathcal{N}}\left(\left|\frac{1}{KN_U}\|\boldsymbol{A}_G\boldsymbol{x}\|_2^2-1\right|\right.\\
&\quad\left.+\left|\frac{1}{KN_U}\|\boldsymbol{A}_E\boldsymbol{y}\|_2^2-1\right|\right), \qquad (98)
\end{aligned}$$

where $\|\cdot\|_2$ denotes the l_2-norm of a vector, and $\mathcal{N}$ denotes the $\frac{1}{4}$-net of the unit sphere S^{N_B-1}, which is a subset of S^{N_B-1} such that for every point $\boldsymbol{x}_0\in S^{N_B-1}$, we can find some point $\boldsymbol{x}\in\mathcal{N}$ so that $\|\boldsymbol{x}-\boldsymbol{x}_0\|_2\le\frac{1}{4}$. Note that (98) follows from the fact that for the $\frac{1}{4}$-net of S^{N_B-1} and the operator norm of any square matrix $\boldsymbol{D}$, $\|\boldsymbol{D}\|\le 2\max_{\boldsymbol{x}\in\mathcal{N}}|\langle\boldsymbol{D}\boldsymbol{x},\boldsymbol{x}\rangle|$ [24], where $\langle\cdot,\cdot\rangle$ denotes the inner product of two vectors. Furthermore, the cardinality of $\mathcal{N}$ satisfies $|\,\mathcal{N}\,|\le 9^{N_B}$. Moreover, we have

$$\|\boldsymbol{A}_G\boldsymbol{x}\|_2^2=\sum_{k=1}^{KN_U}|\,\Phi_k\,|^2, \qquad (99)$$

$$\|\boldsymbol{A}_E\boldsymbol{y}\|_2^2=\sum_{k=1}^{KN_U}|\,\Psi_k\,|^2, \qquad (100)$$

where

$$\Phi_k\triangleq\sum_{s=1}^{N_B}Z_G^{i_k+1}(s,k-i_kN_U)^*x_s, \qquad (101)$$

$$\text{and}\quad\Psi_k\triangleq\sum_{s=1}^{N_B}Z_E^{i_k+1}(s,k-i_kN_U)^*y_s, \qquad (102)$$

with $i_k = \lceil \frac{k}{N_U} \rceil - 1$ and $(\cdot)^*$ denoting the complex conjugate operation. Because the entries of $\boldsymbol{Z}_G$ are zero-mean Gaussian variables and the entries of $\boldsymbol{Z}_E$ are are the linear combination of zero-mean sub-exponential variables, it then follows that Φ_k is the linear combination of Gaussian variables and Ψ_k is the linear combination of sub-exponential variables. The Hoeffding-type inequality and the Bernstein-type inequality characterize the distribution of the linear combination of different types of zero-mean random variables with decaying pdf [24]. In particular, we have

$$\mathrm{P}\{|\ \Phi_k\ | \geq q\} \leq \exp\left(1 - \frac{q^2}{\phi_k^2}\right), \tag{103}$$

$$\text{and} \quad \mathrm{P}\{|\ \Psi_k\ | \geq q\} \leq \exp\left(1 - \min\left(\frac{q^2}{\psi_k^2}, \frac{q}{\psi_k}\right)\right), \tag{104}$$

where ϕ_k is the sub-Gaussian norm of the vector $[Z_G^{i_k+1}(s, k - i_k N_U), s = 1, \ldots, N_B]$, given by

$$\phi_k \triangleq \max_s \min_{p \geq 1} p^{-\frac{1}{2}} \left(\mathbb{E}|Z_G^{i_k+1}(s, k - i_k N_U)|^p\right)^{\frac{1}{p}}; \tag{105}$$

whereas ψ_k is the sub-exponential norm of the vector $[Z_E^{i_k+1}(s, k - i_k N_U), s = 1, \ldots, N_B]$, given by

$$\psi_k \triangleq \max_s \min_{p \geq 1} p^{-1} \left(\mathbb{E}|Z_E^{i_k+1}(s, k - i_k N_U)|^p\right)^{\frac{1}{p}}. \tag{106}$$

According to Lemma 2 and the definition of sub-Gaussian and sub-exponential random variables [24], ϕ_k and ψ_k can be computed as follows:

$$\phi_k = \sqrt{2} e \mathrm{var}\{Z_G(1, k)\}, \tag{107}$$

$$\text{and} \quad \psi_k = e\sqrt{\mathrm{var}\{Z_E(1, k)\}}, \tag{108}$$

where $\mathrm{var}\{Z_G(1, k)\}$ and $\mathrm{var}\{Z_E(1, k)\}$ are given by (75)–(76). Thus Φ_k is a sub-Gaussian random variable and the decaying rate of the pdf of Ψ_k is at least sub-exponential.

Define $\epsilon \triangleq \max(\delta, \delta^2)$ and $\delta \triangleq c_3\sqrt{\frac{2N_B}{KN_U}} + \frac{q}{\sqrt{KN_U}}$, where c_3 is a constant that will be set later. If we set δ in Lemma 1 in this way, we can find that δ is small when K is large, which means the bounds become tighter as K increase. Furthermore, from the later analysis, the probability in (96) becomes smaller as K increases. We have (109)

$$\begin{aligned}
&\mathrm{P}\left\{\left|\frac{1}{KN_U}\|\boldsymbol{A}_G\boldsymbol{x}\|_2^2 - 1\right| + \left|\frac{1}{KN_U}\|\boldsymbol{A}_E\boldsymbol{y}\|_2^2 - 1\right| \geq \epsilon\right\} \\
&\leq \mathrm{P}\left\{\left(\left|\frac{1}{KN_U}\sum_{k=1}^{KN_U}(|\ \Phi_k\ |^2 - 1)\right| \geq \frac{\epsilon}{2}\right)\right. \\
&\qquad \left. \cup \left(\left|\frac{1}{KN_U}\sum_{k=1}^{KN_U}(|\ \Psi_k\ |^2 - 1)\right| \geq \frac{\epsilon}{2}\right)\right\} \\
&= \mathrm{P}\left\{\left|\frac{1}{KN_U}\sum_{k=1}^{KN_U}(|\ \Phi_k\ |^2 - 1)\right| \geq \frac{\epsilon}{2}\right\} \\
&\quad + \mathrm{P}\left\{\left|\frac{1}{KN_U}\sum_{k=1}^{KN_U}(|\ \Psi_k\ |^2 - 1)\right| \geq \frac{\epsilon}{2}\right\}.
\end{aligned} \tag{109}$$

In addition, when $K \to \infty$, for the tall matrices $\boldsymbol{A}_G$ and $\boldsymbol{A}_E$ we have $\mathbb{E}\{|\ \Phi_k\ |^2\} \to 1$ and $\mathbb{E}\{|\ \Psi_k\ |^2\} \to 1$ [24], which means $|\ \Phi_k\ |^2 - 1$ and $|\ \Psi_k\ |^2 - 1$ tend to zero-mean random variables.

Since $\{\Phi_k\}$ are sub-Gaussian, so $\{|\ \Phi_k\ |^2 - 1\}$ are sub-exponential random variables. Therefore according to the Bernstein-type inequality,

$$\begin{aligned}
&\mathrm{P}\left\{\left|\frac{1}{KN_U}\sum_{k=1}^{KN_U}(|\ \Phi_k\ |^2 - 1)\right| \geq \frac{\epsilon}{2}\right\} \\
&\leq 2\exp\left[-KN_U \max\left(\frac{K}{K_G^4}, \frac{K}{K_G^2}\right)\min(\epsilon, \epsilon^2)\right] \\
&= 2\exp\left[-KN_U \max\left(\frac{K}{K_G^4}, \frac{K}{K_G^2}\right)\delta^2\right] \\
&\leq 2\exp\left[-\max\left(\frac{K}{K_G^4}, \frac{K}{K_G^2}\right)\left(2c_3^2 N_B + q^2\right)\right],
\end{aligned} \tag{110}$$

where K_G is the sub-Gaussian norm of the vector $[\Phi_k, k = 1, \ldots, KN_U]$, and

$$K_G = \max_{k=1,\ldots,KN_U}(2e^3 \mathrm{var}^2\{Z_G(1, k)\}). \tag{111}$$

Similarly by (104) and the Bernstein-type inequality, we have

$$\begin{aligned}
&\mathrm{P}\left\{\left|\frac{1}{KN_U}\sum_{k=1}^{KN_U}(|\ \Psi_k\ |^2 - 1)\right| \geq \frac{\epsilon}{2}\right\} \\
&\leq 2\exp\left[-KN_U \max\left(\frac{K}{K_E^2}, \frac{K}{K_E}\right)\min(\epsilon, \sqrt{\epsilon})\right] \\
&= 2\exp\left[-KN_U \max\left(\frac{K}{K_E^2}, \frac{K}{K_E}\right)\delta\right] \\
&\leq 2\exp\left[-\max\left(\frac{K}{K_E}, \frac{K}{K_E^2}\right)\right. \\
&\qquad \left. \times\left(c_3\sqrt{2KN_B N_U} + q\sqrt{KN_U}\right)\right],
\end{aligned} \tag{112}$$

where K_E is the sub-exponential norm of the vector $[\Psi_k, k = 1, \ldots, KN_U]$, and

$$K_E = \max_{k=1,\ldots,KN_U}(e^2\sqrt{2\mathrm{var}\{Z_E(1, k)\}}). \tag{113}$$

We define $c_E \triangleq K\max(\frac{1}{K_E}, \frac{1}{K_E^2})$ and $c_G \triangleq K\max(\frac{1}{K_G^4}, \frac{1}{K_G^2})$. According to the feature of $\mathcal{N}$, we have $|\ \mathcal{N}\ | \leq 9^{N_B}$. Therefore when we choose sufficiently large c_3 satisfying

$$c_3 \geq 2\max\left(\sqrt{\frac{\log 9}{c_G}}, 2\sqrt{\frac{2N_B}{KN_U}\frac{\log 9}{c_E}}\right), \tag{114}$$

we have

$$\begin{aligned}
&\mathrm{P}\left\{\max_{\boldsymbol{x},\boldsymbol{y}\in\mathcal{N}}\left(\left|\frac{1}{KN_U}\|\boldsymbol{A}_G\boldsymbol{x}\|_2^2 - 1\right|\right.\right. \\
&\qquad \left.\left. + \left|\frac{1}{KN_U}\|\boldsymbol{A}_E\boldsymbol{y}\|_2^2 - 1\right|\right) \geq \epsilon\right\} \\
&\leq |\ \mathcal{N}\ |^2 \left\{2\exp\left[-c_G(2c_3^2 N_B + q^2)\right]\right. \\
&\qquad \left. + 2\exp[-c_E(c_3\sqrt{2KN_B N_U} + \sqrt{KN_U}q)]\right\} \\
&\leq 2[\exp(-c_E\sqrt{KN_U}q) + \exp(-c_G q^2)],
\end{aligned} \tag{115}$$

and

$$\begin{aligned}
&\sqrt{2KN_U} - 2c_3\sqrt{N_B} - \sqrt{2}q \\
&\quad \leq s_{\boldsymbol{A}} \leq \sqrt{2KN_U} + 2c_3\sqrt{N_B} + \sqrt{2}q.
\end{aligned} \tag{116}$$

If the lower bound of (116) is positive, we can obtain (47). This completes the proof.

REFERENCES

[1] S. Borade, L. Zheng, and R. Gallager, "Amplify-and-foward in wireless relay networks: Rate, diversity and network size," *IEEE Trans. Inf. Theory*, vol. 53, no. 10, pp. 3302–3318, Oct. 2007.

[2] N. Fawaz, K. Zarifi, M. Debbah, and D. Gesbert, "Asymptotic capacity and optimal precoding in MIMO multi-hop relay networks," *IEEE Trans. Inf. Theory*, vol. 57, no. 4, pp. 2050–2069, Apr. 2011.

[3] J. Hoydis, R. Couillet, and M. Debbah, "Iterative deterministic equivalents for the performance analysis of communication systems," , 2011 [Online]. Available: http://arxiv.org/abs/1112.4167, arXiv Preprint: 1112.4167.

[4] C.-K. Wen, J.-C. Chen, and P. Ting, "Robust transmitter design for amplify-and-forward MIMO relay systems exploiting only channel stastics," *IEEE Trans. Wireless Commun.*, vol. 11, no. 2, pp. 668–682, Feb. 2012.

[5] R. Mo and R. H. Chew, "Precoder design for non-regenerative MIMO relay systems," *IEEE Trans. Wireless Commun.*, vol. 8, no. 10, pp. 5041–5049, Oct. 2009.

[6] O. Munoz, J. Vidal, and A. Agustin, "Linear transceiver design in nonregenerative relays with channel state information," *IEEE Trans. Signal Process.*, vol. 55, no. 6, pp. 2593–2604, Jun. 2007.

[7] R. Rolny, J. Wagner, C. Esli, and A. Wittneben, "Distributed gain matrix optimization in non-regenerative MIMO relay networks," in *Proc. Asilomar Conf. Signals Syst. Comp.*, Pacific Grove, CA, USA, 2009, pp. 1503–1507.

[8] X. Tang and Y. Hua, "Optimal design of non-regenerative MIMO wireless relays," *IEEE Trans. Wireless Commun.*, vol. 6, no. 4, pp. 1398–1407, Apr. 2007.

[9] Y. Ding, J.-K. Zhang, and K. M. Wong, "Ergodic channel capacities for the amplify-and-forward half-duplex cooperative systems," *IEEE Trans. Inf. Theory*, vol. 55, no. 2, pp. 713–730, Feb. 2009.

[10] N. Jindal, S. Vishwanath, and A. Goldsmith, "On the duality of Gaussian multiple-access and broadcast channels," *IEEE Trans. Inf. Theory*, vol. 50, no. 5, pp. 768–783, May 2004.

[11] D. Gesbert, S. Hanly, H. Huang, S. S. Shitz, O. Simeone, and W. Yu, "Multi-cell MIMO cooperative networks: A new look at interference," *IEEE J. Sel. Areas Commun.*, vol. 28, no. 9, pp. 1380–1408, Dec. 2010.

[12] S. Chatzinotas, M. A. Imran, and R. Hoshyar, "On the multicell processing capacity of the cellular MIMO uplink channel in correlated Rayleigh fading environment," *IEEE Tran. Wireless Commun.*, vol. 8, no. 7, pp. 3704–3715, Jul. 2009.

[13] O. Simeone, O. Somekeh, Y. Bar-Ness, and U. Spagnolini, "Uplink throughput of TDMA cellular systems with multi-cell processing and amplify-and-foward cooperation between mobiles," *IEEE Trans. Wireless Commun.*, vol. 6, no. 8, pp. 2942–2951, Aug. 2007.

[14] J. P. Kermoal, L. Schumacher, K. I. Pedersen, P. E. Mogensen, and F. Frederiksen, "A stochastic MIMO radio channel model with experimental validation," *IEEE J. Sel. Areas Commun.*, vol. 20, no. 6, pp. 1211–1226, Aug. 2002.

[15] E. Visotsky and U. Madhow, "Space-time transmit precoding with imperfect feedback," *IEEE Trans. Inf. Theory*, vol. 47, no. 6, pp. 2632–2639, Sep. 2001.

[16] J. C. Roh and B. D. Rao, "Efficient feedback methods for MIMO channels based on parameterization," *IEEE Trans. Wireless Commun.*, vol. 6, no. 1, pp. 282–292, Jan. 2007.

[17] M. A. Sadrabadi, A. K. Khandani, and F. Lahouti, "Channel feedback quantization for high data rate MIMO systems," *IEEE Trans. Wireless Commun.*, vol. 5, no. 12, pp. 3335–3338, Dec. 2006.

[18] D. J. Love and R. W. Heath, "Limited feedback unitary precoding for spatial multiplexing systems," *IEEE Trans. Inf. Theory*, vol. 51, no. 8, pp. 2967–2976, Aug. 2005.

[19] B. M. Hochwald, T. L. Marzetta, T. J. Richardson, W. Sweldens, and R. Urbanke, "Systematic design of unitary space-time constellations," *IEEE Trans. Inf. Theory*, vol. 46, no. 6, pp. 1962–1973, Sep. 2000.

[20] R. Couillet, M. Debbah, and J. W. Silverstein, "A deterministic equivalent for the analysis of correlated MIMO multiple access channels," *IEEE Trans. Inf. Theory*, vol. 57, no. 6, pp. 3493–3514, Jun. 2011.

[21] J. Zhang, C.-K. Wen, S. Jin, X. Gao, and K.-K. Wong, "On capacity of large-scale MIMO multiple access channels with distributed sets of correlated antennas," *IEEE J. Sel. Areas Commun.*, vol. 31, no. 2, pp. 133–148, Feb. 2013.

[22] A. M. Tulino and S. Verdu, *Random Matrix Theory and Wireless Communications*. New York, NY, USA: Now , 2004, vol. 1, no. 1.

[23] V. L. Girko, *Theory of Random Determinants*. Boston, MA, USA: Kluwer Academic , 1990.

[24] R. Vershynin, "Introduction to the non-asymptotic analysis of random matrices," in *Compressed Sensing: Theory and Applications*. Cambridge, U.K.: Cambridge Univ. Press, 2012, pp. 210–268, ch. 5.

[25] W. Weichselberger, M. Herdin, H. Ozcelik, and E. Bonek, "A stochastic MIMO channel model with joint correlation of both link ends," *IEEE Trans. Wireless Commun.*, vol. 5, no. 1, pp. 90–100, Jan. 2006.

[26] L. Liu, R. Chen, S. Geirhofer, K. Sayana, Z. Zhi, and Y. Zhou, "Downlink MIMO in LTE-Advanced: SU-MIMO vs. MU-MIMO," *IEEE Commun. Mag.*, vol. 50, no. 2, pp. 140–147, Feb. 2012.

[27] *Technical specification group radio access network; physical channels and modulation (release 8)*, 3GPP, 36.211, May 2009.

Hao Wu received the B.S. degree in mathematics and applied mathematics from Beijing University of Posts and Telecommunications, Beijing, China, in 2010.

He is currently working toward the Ph.D. degree in communication and signal processing with the School of Information Science and Engineering, Southeast University, Nanjing, China. He was a visiting student at Columbia University, New York, during 2011–2012. His research interests include MIMO wireless communications, large scale antenna array systems, and iterative signal processing.

Liming Wang (S'08–M'11) received the B.S. degree in electronic engineering from the Huazhong University of Science and Technology, China, in 2006, the M.S. degree in mathematics, and the Ph.D. degree in electrical and computer engineering from the University of Illinois at Chicago, both in 2011.

From January 2011 to April 2012, he was a Postdoctoral Research Scientist in the Department of Electrical Engineering, Columbia University, New York. Since May 2012, he has been a Postdoctoral Associate in the Department of Electrical and Computer Engineering, Duke University. His research interests are in high-dimensional data processing; machine learning; statistical signal processing; compressive sensing; bioinformatics and genomic signal processing.

Xiaodong Wang (S'98–M'98–SM'04–F'08) received the Ph.D. degree in electrical engineering from Princeton University.

He is a Professor of Electrical Engineering at Columbia University, New York. His research interests fall in the general areas of computing, signal processing and communications, and has published extensively in these areas. Among his publications is a book entitled *Wireless Communication Systems: Advanced Techniques for Signal Reception* (Englewood Cliffs, NJ: Prentice-Hall, 2003). His current research interests include wireless communications, statistical signal processing, and genomic signal processing.

Dr. Wang received the 1999 NSF CAREER Award, the 2001 IEEE Communications Society and Information Theory Society Joint Paper Award, and the 2011 IEEE Communication Society Award for Outstanding Paper on New Communication Topics. He has served as an Associate Editor for the IEEE TRANSACTIONS ON COMMUNICATIONS, the IEEE TRANSACTIONS ON WIRELESS COMMUNICATIONS, the IEEE TRANSACTIONS ON SIGNAL PROCESSING, and the IEEE TRANSACTIONS ON INFORMATION THEORY. He is listed as an ISI Highly-cited Author.

Xiaohu You (SM'11–F'12) received the B.S., M.S., and Ph.D. degrees in electrical engineering from Nanjing Institute of Technology, Nanjing, China, in 1982, 1985, and 1989, respectively.

From 1987 to 1989, he was with the Nanjing Institute of Technology as a Lecturer. From 1990 to the present, he has been with Southeast University, first as an Associate Professor and later as a Professor. His research interests include mobile communications, adaptive signal processing, and artificial neural networks with applications to communications and biomedical engineering. He is the Chief of the Technical Group of China 3G/B3G Mobile Communication R&D Project.

Dr. You received the excellent paper prize from the China Institute of Communications in 1987, the Elite Outstanding Young Teacher Awards from Southeast University in 1990, 1991, and 1993, and the National Technological Invention Award of China in 2011. He was also a recipient of the 1989 Young Teacher Award of Fok Ying Tung Education Foundation, State Education Commission of China.